UC Berkeley
UC Berkeley Previously Published Works

Title
n-Butane dehydrogenation over Pt/Mg(In)(Al)O

Permalink
https://escholarship.org/uc/item/87c001qt

Authors
Wu, Jason
Peng, Zhenmeng
Sun, Pingping
et al.

Publication Date
2014

DOI
10.1016/j.apcata.2013.10.058

Peer reviewed

eScholarship.org Powered by the California Digital Library
University of California

Applied Catalysis A: General 470 (2014) 208–214

Contents lists available at ScienceDirect

Applied Catalysis A: General

journal homepage: www.elsevier.com/locate/apcata

n-Butane dehydrogenation over Pt/Mg(In)(Al)O

Jason Wu, Zhenmeng Peng, Pingping Sun, Alexis T. Bell*

Department of Chemical and Biomolecular Engineering, University of California, Berkeley, CA 94720-1642, USA

ARTICLE INFO

Article history:
Received 5 August 2013
Received in revised form 26 October 2013
Accepted 29 October 2013
Available online 5 November 2013

Keywords:
Butane dehydrogenation
Pt bimetallic catalysts
Mg(In)(Al)O
Coke formation

ABSTRACT

The thermal dehydrogenation of butane to butene and hydrogen was investigated over Pt nanoparticles supported on calcined hydrotalcite containing indium, Mg(In)(Al)O. Prior work has shown that upon reduction in H_2 at temperatures above 673 K, bimetallic Pt-In particles of are formed, as evidenced by XANES and EXAFS. The performance of Pt/Mg(In)(Al)O for butane dehydrogenation was found to be highly dependent on the bulk In/Pt ratio. The optimal ratio was found to be between 0.33 and 0.88, yielding >95% selectivity to butenes. Hydrogen co-fed with butane was shown to suppress coke formation and catalyst deactivation, a ratio of $H_2/C_4H_{10} = 2.5$ providing the best catalytic performance. Regeneration of catalysts after removal of accumulated carbon and reduction in H_2 restored the original catalyst activity and selectivity. Butane dehydrogenation above 803 K resulted in higher formation of butadiene, a known precursor to coke. No evidence for butane cracking was found to occur on Pt/Mg(In)(Al)O due to moderately basic nature of the support. The present study shows that Pt/Mg(In)(Al)O exhibits superior performance for butane dehydrogenation compared to supported Pt catalysts promoted with Sn, Ge, Pb, and In prepared by successive incipient wetness impregnation of the Pt and promoter precursors.

© 2013 Elsevier B.V. All rights reserved.

1. Introduction

Light alkenes, such as ethene, propene, and butene, are widely use as building blocks for the production of rubber, plastics, and other polymers [1]. Light alkenes are currently produced by steam cracking of alkanes or naphtha at high temperatures. However, these processes exhibit low alkene selectivity and produce significant amounts of methane and coke. Catalytic dehydrogenation of C_2–C_5 alkanes offers an attractive alternative because it utilizes low-cost reactants and can be carried out with high selectivity [2]. Hydrogen is a desirable byproduct that can be used in processes such as hydrocracking and hydrodesulfurization. Since the dehydrogenation of alkanes is endothermic, high temperatures are required to achieve reasonable conversions. The heat required for alkane dehydrogenation can be supplied externally through the combustion of methane or, alternatively, through the combustion of a portion of the hydrogen generated by alkane dehydrogenation [3].

Platinum is known to be the most effective transition metal for dehydrogenation of light alkanes. However, in the absence of a promoting element, platinum catalysts exhibit low alkene selectivity and deactivate rapidly due to coke formation. Addition of a modifying element such as Sn, Zn, Ge, Ga, or In, to form a bimetallic alloy with Pt [4–12], increases the alkene selectivity and decreases the formation of coke [13–17]. Studies of Pt bimetallic alloys suggest that the promoting element enhances the dissociative adsorption of the reacting alkane and reduces the adsorption of the product alkene, the process that initiates coke formation [18–21]. The support composition can also affect the sintering of the supported metal and the formation of coke. Studies have shown that metal oxide supports free of acid sites, such as K–L zeolite, spinels, akali-doped alumina, and calcined hydrotalcite, reduce coke formation [13,22–28]. Mg(Al)O, or calcined hydrotalcite-like material, is particularly attractive because it is moderately basic and thermally stable. The Al cations in the support help to maintain the dispersion of Pt [29].

The modifying element studied most extensively is Sn [17,30–37]. Supported Pt-Sn catalysts are commonly synthesized by coimpregnation of Pt and Sn precursors into a metal oxide support. Properties of the PtSn catalyst depend heavily on composition of precursors and synthesis procedure [17]. Pt-In catalysts, however, have been found to have narrower particle size distributions and more uniform composition than Pt-Sn catalysts [38,39]. We have recently shown a novel approach for producing Pt-Ga and Pt-In bimetallic nanoparticles supported on calcined hydrotalcite containing Ga or In [40,41]. These catalysts exhibit high activity and selectivity for ethane and propane dehydrogenation. Characterization of these catalysts by XANES and EXAFS has shown that during H_2 reduction at 873 K, a part of the Ga^{3+} or In^{3+} cations at the surface of the support is reduced and the resulting zero-valent Ga or In forms Pt–Ga or Pt-In bimetallic particles [40,41].

While butenes are valuable products, the production of butene by butane dehydrogenation has not been studied as extensively and systematically as the production of C_2 or C_3 alkenes by

* Corresponding author.
E-mail address: alexbell@uclink.berkeley.edu (A.T. Bell).

0926-860X/$ – see front matter © 2013 Elsevier B.V. All rights reserved.
http://dx.doi.org/10.1016/j.apcata.2013.10.058

dehydrogenation of the corresponding alkanes. Table 1 lists previous studies of n-butane dehydrogenation over Pt-containing bimetallic catalysts under various reaction conditions. It is notable that some of the previous studies [42,43] were carried out under conditions close to thermodynamic equilibrium. Consequently, it is not possible to gauge the intrinsic activity of the catalysts reported or the effects of time on stream on catalyst activity. Here, we report the performance of Pt/Mg(In)(Al)O catalyst for the dehydrogenation of n-butane. Reaction conditions were chosen such that the catalyst operated away from thermodynamic equilibrium, enabling us to investigate the effects of In/Pt ratio on the intrinsic activity, butene selectivity, stability, and coking of Pt/Mg(In)(Al)O.

2. Experimental

2.1. Catalyst preparation

The support, Mg(In)(Al)O, was prepared by the following procedure. 58.31 g of $Mg(NO_3)_2{\cdot}6H_2O$ (Alfa Aesar, 98–102%), appropriate amounts (depending on the desired In/Al ratio) of $Al(NO_3)_3{\cdot}\,9H_2O$ (Alfa Aesar, 98–102%) and $In(NO_3)_3{\cdot}xH_2O$ (Alfa Aesar, 99.9%), were dissolved in 250 mL of deionized water. A second solution containing 1.2 g of Na_2CO_3 (EMD Chemicals Inc, 99.5%) and 11 g of NaOH (Fisher Scientific, 98.3%) was prepared in 250 ml deionized water. The two solutions were mixed drop-wise with stirring, at 333 K in 20 min, and aged at room temperature for 18 h. The resulting suspension was filtered, and the solid product dried in air overnight at 383 K. This product was then heated in air to 973 K at 2 K/min and maintained at this temperature for 10 h to obtain the calcined hydrotalcite-like support, Mg(In)(Al)O.

Pt was dispersed onto 1 g of Mg(In)(Al)O by incipient wetness impregnation, using a solution containing 21 mg of Pt(acetylacetonate)$_2$ (Sigma Aldrich, 99.99%) dissolved in 1.5 mL toluene. The mixture was then left at room temperature in air for 2 h, and dried overnight at 383 K in an oven. After drying, the catalyst was reduced at 723 K for 2 h in 10% H_2/Ar (60 cm^3/min). The content of Pt, Mg, Al and In was determined by Galbraith Laboratories (Knoxville, TN) using inductively coupled plasma optical emission spectroscopy with samples dissolved in hydrofluoric acid.

2.2. Catalyst testing

Reactions were carried out in a quartz reactor with an inner diameter of 7 mm. Prior to testing, the catalyst (0.005 g, 0.25–0.5 mm particle size, diluted with quartz particles of the same particle size in a 1:4 ratio) was heated at 10 K/min to 873 K in 20% H_2 in He (100 cm^3/min) and then maintained at this temperature for 1 h. The catalyst bed was heated by a three-zone furnace (Applied Test System, Inc.) controlled by Watlow 998 controllers. The temperature of the catalyst bed was measured by two thermocouples centered axially inside the reactor, one at the top and one at the bottom of the catalyst bed. Brooks mass flow controllers were used to deliver each gas. All experiments were performed in the kinetic regime. The absence of intra-particle mass transport effects was evidenced by a linear Arrhenius plot and was further confirmed using the Weisz-Prater criterion.

Catalysts were regenerated by oxidization in a flow of 5 vol% O_2 in He (100 cm^3/min) for 15 min followed by reduction in a flow of 20 vol% H_2 in He (100 cm^3/min). Prior the changing gas composition, the reactor was flushed with helium. The amount of coke deposited during 2 h of butane dehydrogenation was determined in the following manner. Upon termination of an experiment, the catalyst was purged in flowing He (60 cm^3/min) at 273 K for 30 min, after which it was exposed to a mixture of 5% O_2 in He flowing at 60 cm^3/min. The CO_2 generated was monitored by online mass

Table 1
N-butane dehydrogenation by Pt-containing bimetallic catalysts. Comparison between conversion at t = 10 min, 2 h and total initial selectivity to all butenes, including butadiene.

Second metal	Support	Pt (wt%)	Size (nm)	T (K)	W/F (g s/cm^3)	%C_4H_{10} Feed	H_2/C_4H_{10}	Initial rate (μmol/g s)	X at t = 10 min	X at t = 2 h	$S_{Butenes}$	Estimated Equil. Conv.	Ref.
Sn	$MgAl_2O_4$	0.3	1–3	803	0.67	44.4	1.25	9.5	32	28	97	22.9	[42]
Pb	$MgAl_2O_4$	0.3	1–3	803	0.67	44.4	1.25	3.9	13	11.3	92	22.9	[42]
Sn	γ–Al_2O_3	0.3	–	803	0.67	44.4	1.25	8.9	30	28	94.4	22.9	[43]
Ge	γ–Al_2O_3	0.3	–	803	0.67	44.4	1.25	8.0	27	18	90.4	22.9	[43]
Sn	SAPO-34	0.5	1.4–2.5	858	2.5	80	0.25	5.1	36.1	13.2	44	58.6	[44]
Sn	CMgO	1	2.8	773	0.2	33.3	1	74.4	17.9	15	95.7	21.5	[45]
In	Mg(Al)(In)O	0.89	1	803	0.00375	13.3	2.5	206	13	7.5	98	35.4	–
In/Sn	$MgAl_2O_4$	0.3	–	803	0.67	44.4	1.25	8.9	30	29	95	22.9	[22]

Table 2
Catalyst composition.

Sample Name	Pt (wt%)	In (wt%)	Starting ratio Mg:Al:In	Mg/(Al + In)*	In/Al*	In/Pt*
Pt/Mg(Al)O	0.70	0	100:10:0	5.09	0	–
Pt/Mg(Al)(In)O-0.33	0.89	0.171	100:9.95:0.05	5.13	0.0047	0.33
Pt/Mg(Al)(In)O-0.48	0.71	0.201	100:9.9:0.10	4.82	0.0065	0.48
Pt/Mg(Al)(In)O-0.88	0.83	0.428	100:9.86:0.14	4.90	0.010	0.88
Pt/Mg(Al)(In)O-1.7	0.67	0.674	100:9.75:0.25	4.60	0.021	1.7

* Determined by ICP–OES.

spectrometry and the amount of coke deposited on catalyst was calculated from the amount of generated CO_2.

Reactants and products were analyzed online using a gas chromatograph–mass spectrometer (Varian, Inc., Model 320) equipped with a 14-port sampling valve and three sample loops. One sample loop was injected into an Alumina PLOT column for flame ionization detection of eluted products. The second sample loop was injected into a second Alumina PLOT column and analyzed by mass spectrometry. The third sample loop was injected into a Hayesep *N* column connected in series with a Mol Sieve 5A packed column, and eluted products were detected by thermal conductivity.

3. Results and discussion

3.1. Effect of addition of In

A list of samples investigated is presented in Table 2. The Pt content was between 0.7–0.8 wt%. The Mg/(Al + In) ratio for the support was maintained at 5, and the In/Al ratio was varied from 0 to 0.083. For all of the catalysts examined, the bulk In/Pt ratio (labeled in the sample name) was between 0 and 1.7. STEM images of Pt/Mg(In)(Al)O show small metal particles about 1 nm in diameter even distributed across the support [41]. Furthermore, similar particle size distributions were observed for all catalysts with In/Pt ratio from 0 to 1.7, suggesting that the presence of In in the support does not affect the metal particle size.

Prior to catalyst testing, empty reactor tests were conducted with reacting gases flowing through reactor without catalyst. It was found that effluent C_1–C_3 (CH_4, C_2H_6, C_2H_4, C_3H_8, C_3H_6) products concentrations formed in the empty reactor were nearly identical to the effluent concentrations observed with a Pt-In catalyst in the reactor from 773 K to 873 K. Therefore, all C_1–C_3 products are taken to arise from the reactor and not the catalyst. This is likely due to the absence of acid sites on Mg(Al)O that would contribute to cracking side reactions. The concentration of these products never exceeded 4% of all products formed at 803 K with $H_2/C_4H_{10} = 2.5$. The selectivities to butenes (1- and 2-butene) were therefore determined from Eq. (1):

$$S_{C4H8}(\%) = [C_4H_8]/([C_4H_8] + [C_4H_6]) \times 100\%, \quad (1)$$

where [*X*] is the molar concentration of *X*.

The effects of In/Pt ratio on conversion and selectivity are shown in Fig. 1. The conversion of *n*-butane goes through a peak in the area between In/Pt = 0.33 and 0.88, while butene selectivity remains above 95% for In/Pt≥0.33. The effect of In/Pt ratio observed in Fig. 1 is similar to that observed for ethane and propane dehydrogenation at 873 K over Pt/Mg(In)(Al)O and Pt/Mg(Ga)(Al)O [40,41]. The occurrence of a maximum in conversion with increasing In/Pt ratio suggests that for In/Pt ratios between 0.33 and 0.88, In incorporation enhances the activity of the catalyst due to an electronic effect on the properties of the Pt atoms present at the particle surface. The decrease in rate for In/Pt ratios above 0.88 is very likely due to a progressive loss in Pt atoms at the particle surface resulting from an increasing fraction of surface In atoms, rather than from

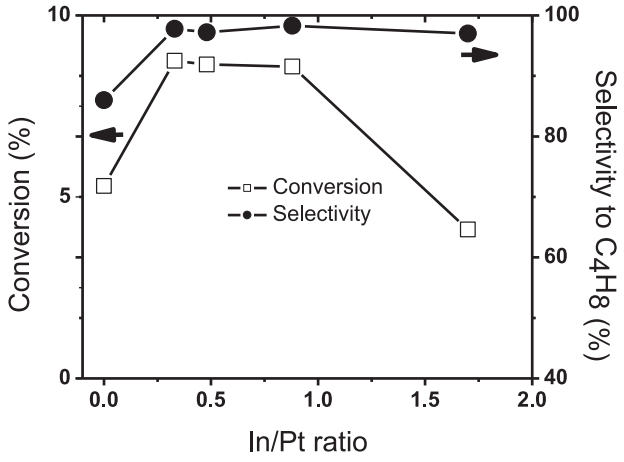

Fig. 1. Effect of In/Pt ratio on butane conversion and butene selectivity after 25 min of time on stream. Reaction conditions: $T = 803$ K, catalyst mass = 5 mg, C_4H_{10}: 13%, total flow rate: 80 cm^3/min, $H_2/C_4H_{10} = 2.5$.

varying particle size distributions across In/Pt ratios. Previous hydrogen chemisorptions experiments show that the percentage of exposed Pt sites for In/Pt = 0.33, 0.48 and 0.88 are 84%, 94%, and 65% respectively [41]. However at In/Pt = 1.7, the percentage of exposed Pt sites drops to 35%, supporting the drop in butane conversion observed here. The increase in selectivity for In/Pt≥0.33 also suggest that the presence of In contributes to the desorption of butenes to prevent the formation of butadiene.

The turnover frequency for butane dehydrogenation was determined based on measurements of H_2 chemisorption [41]. Fig. 2 shows that the TOF for butane dehydrogenation increases by a

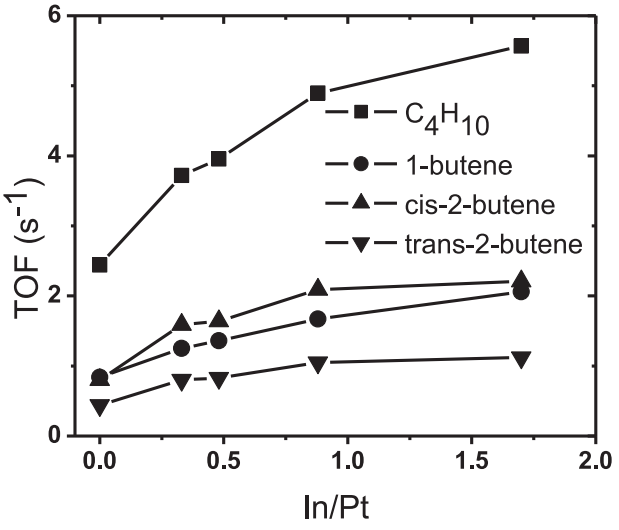

Fig. 2. Effect of In/Pt ratio on butane and butene TOF's after 25 min of time on stream. Reaction conditions: $T = 803$ K, catalyst mass = 5 mg, C_4H_{10}: 13%, total flow rate: 80 cm^3/min, $H_2/C_4H_{10} = 2.5$.

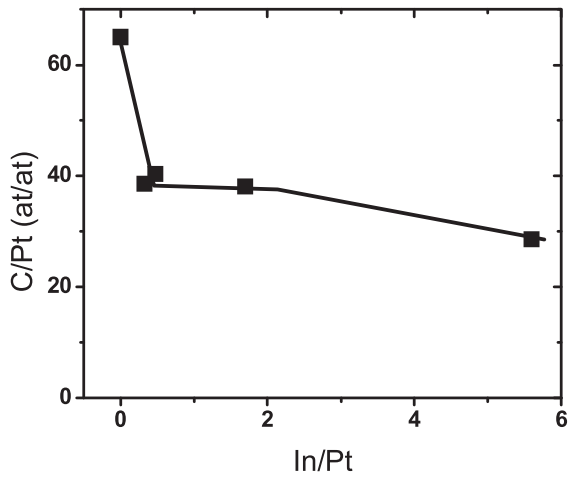

Fig. 3. Dependence of C/Pt ratio on bulk In/Pt ratio measured for 2 h time on stream for butane dehydrogenation on Pt/Mg(In)(Al)O. Reaction conditions: T = 803 K, catalyst mass = 5 mg, C_4H_{10}: 13%, total flow rate: 80 cm^3/min, H_2/C_4H_{10} = 2.5.

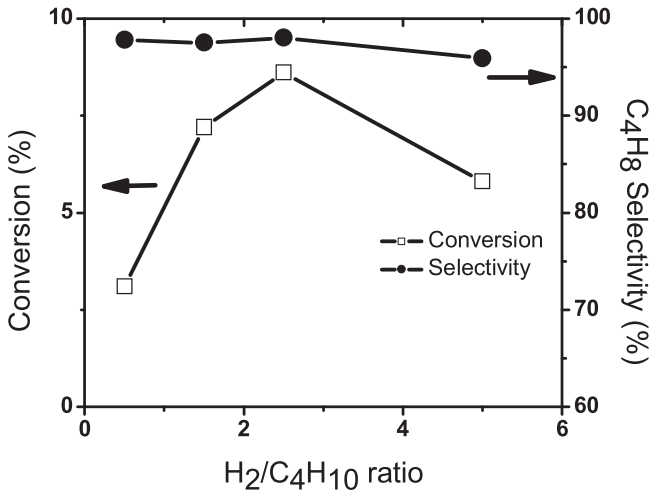

Fig. 4. Effect of hydrogen to n-butane feed ratio on butane over Pt/Mg(In)(Al)O (In/Pt = 0.33) measured after 25 min of time on stream. Total flow kept constant at 80 cm^3/min by adding a balance of He, T = 803 K, catalyst mass = 5 mg, C_4H_{10}: 13%.

factor of two as In/Pt increases from 0 to 1.7. This trend is in agreement with TOF measurements for ethane and propane dehydrogenation over Pt/Mg(In)(Al)O and similar to that observed for ethane dehydrogenation on bimetallic PtSn/Mg(Al)O catalyst [46]. Even though higher In/Pt ratios were not tested beyond 1.7, we surmise that the TOF will eventually decrease beyond In/Pt = 1.7 due to increasing Pt-In coordination on the surface as was seen for ethane and propane dehydrogenation over Pt/Mg(In)(Al)O [41]. Fig. 2 also shows that the distribution of butene isomers was roughly 40% cis-2-butene, 35% 1-butene, and 25% trans-2-butene and was nearly constant across the In/Pt ratios examined.

Carbon accumulation after 2 h of reaction is also a strong function of In/Pt ratio of the catalyst, as shown in Fig. 3. Increasing the In/Pt ratio from 0 to 0.33, causes the C/Pt ratio to decrease by 40%. Similar effects have been observed for ethane and propane dehydrogenation over Pt/Mg(In)(Al)O [41]. The suppression of coke formation by supported bimetallic catalysts, such as Pt-Sn or Pt-In, has been attributed to both geometric and electronic effects. For Pt-Sn catalysts, the presence of Sn at the surface reduces the number of adjacent Pt atoms, hence decreasing the number of Pt atoms in ensembles required to form coke precursors [47]. This same explanation has been proposed for Pt-In catalysts [41]. Since it has been shown that Sn reduces the heat of adsorption of the formed alkene [18–21], it is also reasonable to suggest that In reduces the heat of adsorption of butene, and hence, the extent of coke formation. Butadiene is a well-known precursor to coke, and therefore can contribute to deactivation of catalyst [48,49]. It is notable that while the thermodynamic driving force for graphene formation per unit of carbon is very similar for n-butene and ethene, we observe a greater extent of deactivation under identical conditions for n-butane than ethane dehydrogenation over Pt/Mg(In)(Al)O (In/Pt = 0.33). This is very likely due to the higher thermodynamic potential of butadiene to form coke.

3.2. Effect of hydrogen co-feed

Fig. 4 illustrates the effects of H_2/C_4H_{10} feed ratio on conversion and butene selectivity for Pt/Mg(In)(Al)O-0.33. Previous studies have shown that catalyst deactivation can be inhibited by addition of H_2, CO_2, H_2/O_2, or H_2O to the feed [50–53]. Raising the ratio of H_2 to C_4H_{10} from 0.5 to 2.5 causes a significant increase in butane conversion while selectivity was nearly constant. However, increasing the ratio above 2.5 caused a decrease in conversion. A similar effect has been observed previously in studies of ethane and propane dehydrogenation on Pt/Mg(Al)O, Pt/Mg(Ga)(Al)O, and Pt/Mg(In)(Al)O [40,41,46]. In all the cases, the rate of alkene formation increases with increasing H_2/alkane ratio and then decreases beyond the maximum. We have previously proposed that at low H_2/alkane, adsorbed H atoms on the catalyst surface contribute to the removal of the second hydrogen atom of the adsorbed alkyl species, resulting in a higher rate of alkene formation [40]. Increased butene production can also be attributed to hydrogen inhibiting deactivation by coke formation, as will be discussed. However, at higher surface concentrations of hydrogen, the conversion will decrease due to hydrogenation of the formed alkene. For butane dehydrogenation over Pt/Mg(In)(Al)O, the optimum H_2/C_4H_{10} ratio was 2.5, where butene formation was maximized and hydrogenation to n-butane was minimized.

The amount of carbon accumulated in 2 h of reaction over Pt/Mg(In)(Al)O-0.33 is shown in Fig. 5, as a function of H_2/C_4H_{10} feed ratio. Without hydrogen in the feed (H_2/C_4H_{10} = 0), the accumulated carbon is very high. After 2 h of time on stream, the absence of hydrogen in the feed produces almost four times more coke than

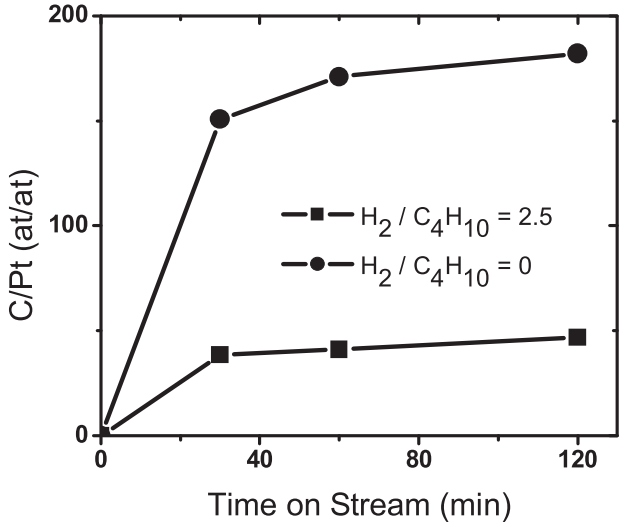

Fig. 5. Amount of coke accumulation with time on stream during butane dehydrogenation on Pt/Mg(In)(Al)O (In/Pt = 0.33) for hydrogen to n-butane feed ratios of 0 and 2.5. Reaction conditions: T = 803 K, catalyst mass = 5 mg, C_4H_{10}: 13%, total flow rate: 80 cm^3/min.

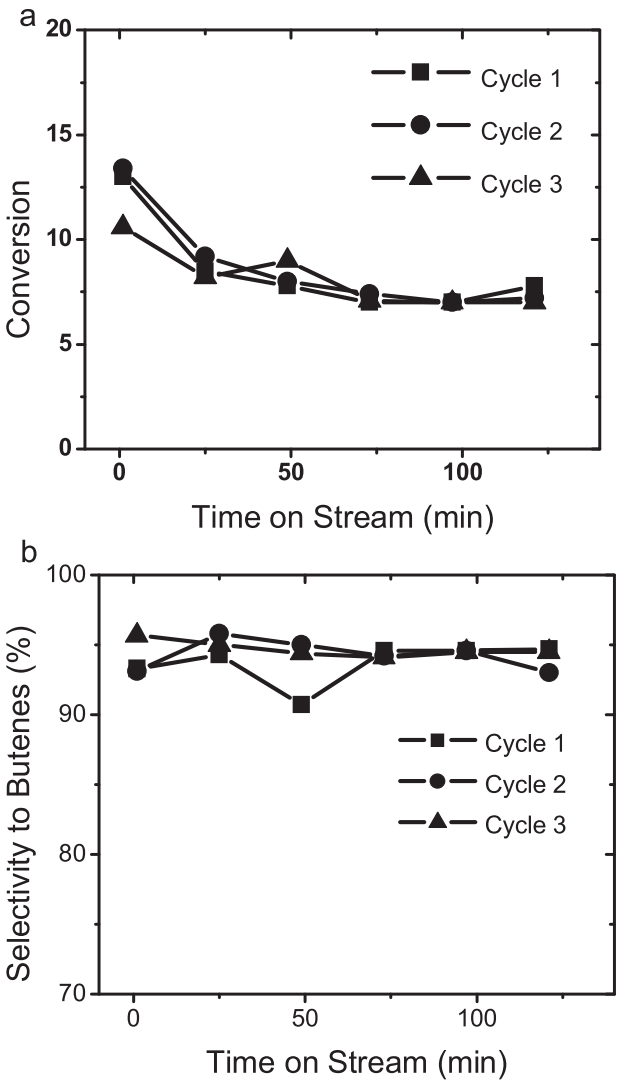

Fig. 6. Effects of catalyst recycling on (a) butane conversion and (b) butene selectivity for butane dehydrogenation over Pt/Mg(In)(Al)O (In/Pt = 0.33). Each cycle consists of reduction-reaction-oxidation steps. Reaction conditions: T = 803 K, catalyst mass = 5 mg, C_4H_{10}: 13%, H_2/C_4H_{10} = 2.5, total flow rate: 80 cm^3/min.

when H_2/C_4H_{10} = 2.5. This trend has been observed previously with PtSn/Mg(Al)O for ethane dehydrogenation [47]. In the presence of hydrogen, the formation of coke precursors, such as butadiene, are suppressed by inhibiting further dehydrogenation of butenes. In addition, it has been shown by TEM for Pt/MgO nanoparticles that graphene layers form rapidly in the first 10 min under ethane dehydrogenation, but reach a plateau afterward [54]. We observe a qualitatively similar behavior during *n*-butane dehydrogenation in that the C/Pt ratio increases rapidly during the first 30 min but then levels off. It is also evident that since the C/Pt ratio is much greater than unity, the majority of the accumulated coke migrates to the support and only a small fraction remain on the surface of the metal particles, allowing access to the surface of the Pt-In nanoparticles.

3.3. Catalyst regeneration

Fig. 6 shows conversion and selectivity for three cycles of butane dehydrogenation over Pt/Mg(In)(Al)O-0.33. After removal of accumulated carbon and H_2 reduction at 873 K, the original conversion and selectivity for butane dehydrogenation is restored close to those seen in Cycle 1. The loss of dehydrogenation activity is minimal between cycles, as also seen for ethane and propane

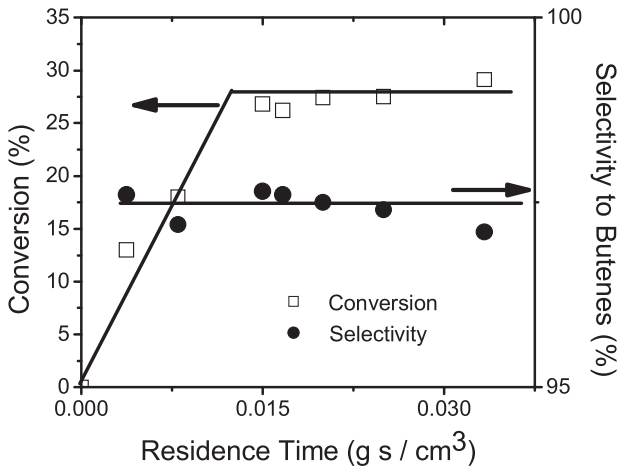

Fig. 7. Effects of residence time (W/F) on *n*-butane conversion and butene selectivity during butane dehydrogenation over Pt/Mg(In)(Al)O (In/Pt = 0.33) measured after 1 min of time on stream. Reaction conditions: T = 803 K, C_4H_{10}: 13%, H_2/C_4H_{10} = 2.5.

dehydrogenation over Pt/Mg(In)(Al)O [41]. Furthermore, deactivation over time on stream is attributed to coke formation rather than sintering. STEM images of reacted Pt/Mg(In)(Al)O show similar particle size distributions after 2 h of ethane and propane dehydrogenation at 873 K [41]. Therefore, we reasonably conclude that sintering is also minimal for butane dehydrogenation, particularly since butane dehydrogenation was carried out at 803 K. During each cycle, the selectivity to butenes is above 95% after 2 h of time on stream.

3.4. Effects of residence time and temperature

The effects of residence time on the conversion of Pt/Mg(In)(Al)O are shown in Fig. 7. At high residence times, the conversion plateaus near 30%, close to that corresponding to equilibrium conversion for the reaction conditions used. All of the data presented in Figs. 1–5 were all performed at 3.75×10^{-3} g s/cm^3, for which the conversion is 13%. At this residence time, the intrinsic rate of n-butane consumption is 206 μmol/g s and the turnover frequency for *n*-butane dehydrogenation is 5.53 s^{-1}, based on H_2 uptake measurements made on Pt/Mg(In)(Al)O (In/Pt = 0.33) [41] to determine the concentration of surface Pt sites. Notably, the selectivity to butenes is constant with residence time.

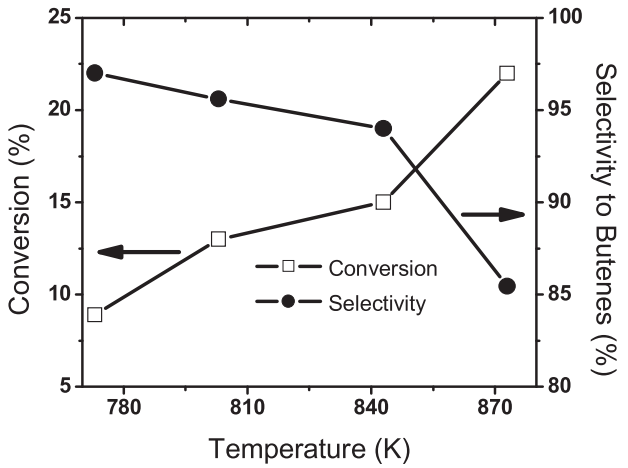

Fig. 8. Effects of temperature on butane conversion and selectivity to butenes for butane dehydrogenation over for Pt/Mg(In)(Al)O (In/Pt = 0.33) measured after 1 min of time on stream. Reaction conditions: catalyst mass = 5 mg, C_4H_{10}: 13%, total flow rate: 80 cm^3/min, H_2/C_4H_{10} = 2.5.

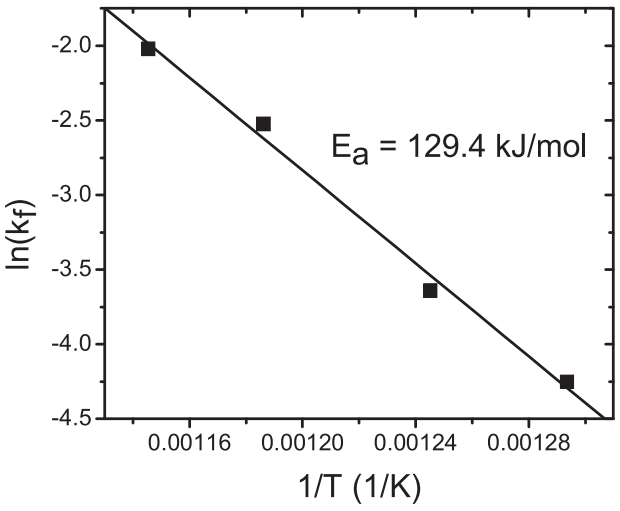

Fig. 9. Plot of $\ln(k_F)$ versus $(1/T)$ determined from conversions and selectivities shown in Fig. 7. Reaction conditions: catalyst mass = 5 mg, C_4H_{10}: 13%, total flow rate = 80 cm^3/min, H_2/C_4H_{10} = 2.5.

The effect of temperature on butane conversion and butene selectivity are shown in Fig. 8. While overall conversion increases with increasing temperature, the selectivity to butenes decreases from 97% at 773 K to 85% at 873 K, the remaining products being butadiene. As noted previously, butadiene is a known precursor to coke, so therefore operation at 873 K leads to significant coke formation and deactivation.

The apparent first-order rate coefficient for butane dehydrogenation, k_f, was determined from the measured rate of reaction corrected for the approach to equilibrium. Fig. 9 shows an Arrhenius plot for k_f. The apparent activation energy determined from this plot is 129.4 kJ/mol, which is similar to the value of 117.2 kJ/mol reported for butane dehydrogenation over PtSn/γ-Al_2O_3 [55].

4. Conclusions

Catalysts for the dehydrogenation of *n*-butane were prepared by dispersing Pt nanoparticles onto a calcined hydrotalcite-like support containing In, Mg(In)(Al)O. Upon reduction at temperatures above 723 K, we have shown previously [41] that a part of the In^{3+} cations present near the support surface and adjacent to Pt are reduced and the resulting In atoms form a Pt-In bimetallic alloy with the supported Pt nanoparticles. Performance of Pt/Mg(In)(Al)O for butane dehydrogenation was a strong function of the bulk In/Pt ratio. Between In/Pt = 0.33 and 0.88, the catalyst activity for butane dehydrogenation reached a maximum and the butene selectivity reaches ~ 95%, with primary products being cis-2-butene and 1-butene. Alloying In with Pt also caused a significant decrease in the accumulation of C during butane dehydrogenation, compared to pure Pt catalyst. We attribute these trends to the geometric and electronic effects from the presence of In, as previously proposed for PtM alloys (M = In, Sn, Ga, Zn, Ge) [4–12,40,41,47]. Addition of hydrogen to the feed also inhibited catalyst deactivation and reduced carbon accumulation, as seen for both ethane and propane dehydrogenation over Pt/Mg(In)(Al)O [41]. Catalyst regeneration by removal of accumulated carbon and subsequent H_2 reduction at 873 K restored the original activity and selectivity. The temperature chosen for butane dehydrogenation was 803 K, above which butadiene formation became increasingly important, resulting in a strong increase in catalyst deactivation due to coking.

Acknowledgment

This work was supported by Chevron Energy Technology Company.

References

[1] J. McGregor, Z. Huang, E.P.J. Parrott, J.A. Zeitler, K.L. Nguyen, J.M. Rawson, A. Carley, T.W. Hansen, J. Tessonnier, D.S. Su, D. Teschner, E.M. Vass, A. Knop-Gericke, R. Scholgl, L.F. Gladden, Journal of Catalysis 269 (2010) 329–339.
[2] D.E. Resasco, Encyclopedia of Catalysis 3 (2002) 49.
[3] J.C. Bricker, Topics in Catalysis 55 (2012) 1309–1314.
[4] P. Sun, G. Siddiqi, M. Chi, A.T. Bell, Journal of Catalysis 274 (2010) 192–199.
[5] L.C. Loc, N.A. Gaidai, S.L. Kiperman, H.S. Thoang, N.M. Podklenova, S.B. Kogan, Kinetiki Kataliz 32 (1991).
[6] N.A. Pakhomov, Kinetics and Catalysis 42 (2001) 334–343.
[7] N. Homs, J. Llorca, M. Riera, J. Jolis, J.-L.G. Fierro, J. Sales, P.R. de la Piscina, Journal of Molecular Catalysis A: Chemical 200 (2003) 251–259.
[8] E.L. Jablonski, A.A. Castro, O.A. Scelza, S.R. de Miguel, Applied Catalysis A: General 183 (1999) 189–198.
[9] O.A. Barias, A. Holmen, E.A. Blekkan, in: B. Delmon, G.F. Froment (Eds.), Catalyst Deactivation, Elsevier Science Publ B V, Amsterdam, 1994, pp. 519–524.
[10] A.A. Castro, Catalysis Letters 22 (1993) 123–133.
[11] S. de Miguel, A. Castro, O. Scelza, J.L.G. Fierro, J. Soria, Catalysis Letters 36 (1996) 201–206.
[12] M. Larsson, B. Andersson, O.A. Barias, A. Holmen, in: B. Delmon, G.F. Froment (Eds.), Catalyst Deactivation, Elsevier Science Publ B V, Amsterdam, 1994, pp. 233–240.
[13] R.D. Cortright, J.M. Hill, J.A. Dumesic, Catalysis Today 55 (2000) 213–223.
[14] A. Virnovskaia, E. Rytter, U. Olsbye, Industrial and Engineering Chemistry Research 47 (2008) 7167–7177.
[15] A.D. Ballarini, C.G. Ricci, M.S.R. de, O.A. Scelza, Catalysis Today 133–135 (2008) 28–34.
[16] L. Bednarova, C.E. Lyman, E. Rytter, A. Holmen, Journal of Catalysis 211 (2002) 335–346.
[17] J. Salmones, J.-A. Wang, J.A. Galicia, G. Aguilar-Rios, Journal of Molecular Catalysis A: Chemical 184 (2002) 203–213.
[18] R. Alcala, J.W. Shabaker, G.W. Huber, M.A. Sanchez-Castillo, J.A. Dumesic, The Journal of Physical Chemistry B 109 (2005) 2074–2085.
[19] J.M. Essen, J. Haubrich, C. Becker, K. Wandelt, Surface Science 601 (2007) 3472–3480.
[20] J. Shen, J.M. Hill, R.M. Watwe, B.E. Spiewak, J.A. Dumesic, The Journal of Physical Chemistry B 103 (1999) 3923–3934.
[21] E. Janin, H. von Schenck, S. Ringler, J. Weissenrieder, T. Åkermark, M. Göthelid, Journal of Catalysis 215 (2003) 245–253.
[22] S.A. Bocanegra, A.A. Castro, O.A. Scelza, S.R. de Miguel, Applied Catalysis A: General 333 (2007) 49–56.
[23] S.A. Bocanegra, A. Guerrero-Ruiz, S.R. de Miguel, O.A. Scelza, Applied Catalysis A: General 277 (2004) 11–22.
[24] M. Tasbihi, F. Feyzi, M.A. Amlashi, A.Z. Abdullah, A.R. Mohamed, Fuel Processing Technology 88 (2007) 883–889.
[25] Y. Zhang, Y. Zhou, A. Qiu, Y. Wang, Y. Xu, P. Wu, Catalysis Communications 7 (2006) 860–866.
[26] T. Waku, J.A. Biscardi, E. Iglesia, Journal of Catalysis 222 (2004) 481–492.
[27] A. Virnovskaia, S. Jørgensen, J. Hafizovic, Ø. Prytz, E. Kleimenov, M. Hävecker, H. Bluhm, A. Knop-Gericke, R. Schlögl, U. Olsbye, Surface Science 601 (2007) 30–43.
[28] A. Virnovskaia, S. Morandi, E. Rytter, G. Ghiotti, U. Olsbye, Journal of Physical Chemistry C 111 (2007) 14732–14742.
[29] J.H. Kwak, J. Hu, D. Mei, C.-W. Yi, D.H. Kim, C.H.F. Peden, L.F. Allard, J. Szanyi, Science 325 (2009) 1670–1673.
[30] H.H.C.M. Pinxt, B.F.M. Kuster, D.C. Koningsberger, G.B. Marin, Catalysis Today 39 (1998) 351–361.
[31] J.M. Ramallo-Lopez, G.F. Santori, L. Giovanetti, M.L. Casella, O.A. Ferretti, F.G. Requejo, The Journal of Physical Chemistry B 107 (2003) 11441–11451.
[32] G.J. Siri, J.M. Ramallo-Lopez, M.L. Casella, J.L.G. Fierro, F.G. Requejo, O.A. Ferretti, Applied Catalysis A: General 278 (2005) 239–249.
[33] R.D. Cortright, J.M. Hill, J.A. Dumesic, Catalysis Today 55 (2000) 213–223.
[34] E. Antolini, F. Colmati, E.R. Gonzalez, Journal of Power Sources 193 (2009) 555–561.
[35] V. Radmilovic, T.J. Richardson, S.J. Chen, P.N. Ross Jr., Journal of Catalysis 232 (2005) 199–209.
[36] N. Nava, P. Del Angel, J. Salmones, E. Baggio-Saitovitch, P. Santiago, Applied Surface Science 253 (2007) 9215–9220.
[37] C. Vértes, E. Tálas, I. Czakó-Nagy, J. Ryczkowski, S. Göbölös, A. Vértes, J. Margitfalvi, Applied Catalysis 68 (1991) 149–159.
[38] M.C. Roman-Martinez, J.A. Macia-Agullo, I.M.J. Vilella, D. Cazorla-Amoros, H. Yamashita, Journal of Physical Chemistry C 111 (2007) 4710–4716.
[39] F.B. Passos, D.A.G. Aranda, M. Schmal, Journal of Catalysis 178 (1998) 478–488.
[40] G. Siddiqi, P. Sun, V. Galvita, A.T. Bell, Journal of Catalysis 274 (2010) 200–206.
[41] P. Sun, G. Siddiqi, W. Vining, M. Chi, A.T. Bell, Journal of Catalysis 282 (2011) 165–174.
[42] S.A. Bocanegra, M.J. Yanez, O. Scelza, S.R. de Miguel, Industrial and Engineering Chemistry Research 49 (2010) 4044–4054.

[43] A.D. Ballarini, P. Zgolicz, I.M.J. Vilella, S.R. de Miguel, A.A. Castro, O.A. Scelza, Applied Catalysis A 381 (2010) 83–91.
[44] Z. Nawaz, W. Fei, Industrial and Engineering Chemistry Research 48 (2009) 7442–7447.
[45] V. Shashikala, H. Jung, C. Shin, H. Koh, K. Jung, Catalysis Letters 143 (2013) 651–656.
[46] J. Wu, Z. Peng, A.T. Bell, Journal of Catalysis (Submitted).
[47] V. Galvita, G. Siddiqi, P. Sun, A.T. Bell, Journal of Catalysis 271 (2010) 209–219.
[48] L.F. Albright, J. Marek, Industrial and Engineering Chemistry Research 27 (1988), 755-599.
[49] L.F. Albright, C.F. McConnell, K. Welther, Thermal Hydrocarbon Chemistry, American Chemical Society, 1979, pp. 175–191.
[50] A. Virnovskaia, E. Rytter, U. Olsbye, Industrial & Engineering Chemistry Research 47 (2008) 7167–7177.
[51] C. Yu, Q. Ge, H. Xu, W. Li, Industrial & Engineering Chemistry Research 46 (2007) 8722–8728.
[52] M. Tasbihi, F. Feyzi, M.A. Amlashi, A.Z. Abdullah, A.R. Mohamed, Fuel Processing Technology 88 (2007) 883–889.
[53] S.B. Kogan, H. Schramm, M. Herskowitz, Applied Catalysis A: General 208 (2001) 185–191.
[54] Z. Peng, F. Somodi, S. Helveg, C. Kisielowski, P. Specht, A.T. Bell, Journal of Catalysis 286 (2012) 22–29.
[55] K. Curry, L.T. Thompson, Catalysis Today 21 (1994) 171–184.